

**SIMULATION OF ROCKET SEEDING OF CONVECTIVE CLOUDS WITH  
COARSE HYGROSCOPIC AEROSOL.  
1. CONDENSATION GROWTH OF CLOUD DROPLETS ON SALT CRYSTALS**

**M.T. Abshaev, A.M. Abshaev, M.K. Zhekamukhov,  
E.I. Potapov\*, I.A. Garaba\*, E.A. Zasavitsky\***

*High Mountain Geophysical Institute of ROSHYDROMET, 2, Lenin ave., 360020, Nalchik,  
Kabardino-Balkaria, Russian Federation*

*E-mail: abshaev@mail.ru*

*\*Institute of Electronic Engineering and Industrial Technologies, Academy of Sciences of  
Moldova, 3/3, Academiei str., MD-2028, Chisinau, Republic of Moldova*

*E-mail: efim@lises.asm.md*

(Received 4 July 2008)

**Abstract**

Laws of aerosol particle distribution at hygroscopic seeding of convective clouds by means of antihail rockets are considered. Influence of salt particle dispersion degree on intensity of condensation growth of separate cloud droplets on these particles is investigated. Analytical formulae describing variation of radius of  $NaCl$  crystal and cloud droplet growing on the salt crystal until its entire dissolution in the droplet are obtained. On the basis of numerical calculations, comparative analysis of salt influence on intensification of condensation growth of droplets in the cloud is carried out.

**1. Statement of the problem**

At present, experiments on seeding of convective clouds with hygroscopic reagents for forced causing or enhancement of precipitation are intensively carried out. Simultaneously, works on optimization of concepts, methods, and facilities for impact on cloud environment are executed. New, more efficient reagents and cheaper facilities for reagent hauling into cloud volumes are actively developed in a number of countries. Experiments with random sampling on hygroscopic seeding of hail clouds carried out in France [6] have shown positive results that require further confirmation and scientific substantiation. Experiments in South Africa, Thailand, and Mexico [5] allowed revealing that hygroscopic seeding of convective clouds causes statistically significant enhancement of precipitation.

At the same time, laws of transformation of macro- and microphysical processes in cloud environment in the course of hygroscopic seeding remain underresearched; that is, how actively simulated particles introduced into cloud environment absorb cloud vapor; how actively growing droplets on hygroscopic particles absorb cloud droplets, and how much time is required for formation of simulated precipitation particles. It is also imperative to select the reagent dose and optimum degree of particle dispersion depending on type of impact on cloud environment; this is necessary for engineering and specification of requirements on impact facilities.

In this paper we present one of the variants of forced influence on cloud environment - hygroscopic seeding of convective clouds by means of antihail rockets. The authors have taken a shot at theoretical study of the laws of transformation of microphysical parameters in seeded volumes and finding a possibility to select optimum degree of dispersion for hygroscopic particles, and further improvement of methods for forced impact on clouds with the aim of precipitation enhancement.

## 2. Turbulent diffusion of aerosol particles in the course of rocket seeding of clouds

Let us discuss the diffusive process in a cloud formed by reactive gases of antihail rockets, considering it an expanding cylinder of infinite extent that contains hygroscopic particles inside, for example,  $NaCl$  particles. Herein, laws of formation of initial primordial aerosol particles and kinetics of formation of their spectrum in reactive gases of antihail rockets are not considered by us. On the basis of experimental data, concentrations and dimensions of hygroscopic particles contained in reactive gases immediately after their discharge from a rocket nozzle are specified. Under these conditions, further distribution of hygroscopic particles in cloud environment may be interpreted as turbulent diffusion of impurities from an instantaneous linear source in the environment with homogeneous isotropic turbulence.

According to the theory of Kolmogorov-Obukhov, the turbulent diffusion coefficient  $K$  will be assigned as  $K = \kappa_1 \varepsilon^{1/3} l^{4/3}$ , where  $\kappa_1$  is a dimensionless constant close to one;  $\varepsilon$  is the rate of turbulent energy;  $l$  is the typical scale of turbulence.

In the course of distribution of impurity from the instantaneous linear source, the turbulent diffusion coefficient grows in proportion to  $r^{4/3}$ , where  $r$  is the cylindrical coordinate ( $2r = l$  is the representative scale of turbulence), and the diffusion equation takes the form

$$\frac{\partial c}{\partial t} = \frac{\kappa \varepsilon^{1/3}}{r} \frac{\partial}{\partial r} \left( r^{7/3} \frac{\partial c}{\partial r} \right), \quad r > 0, \quad (1)$$

where  $c$  is the particle concentration;  $t$  is the time;  $\kappa = \frac{\kappa_1}{2^{4/3}} \approx 0,4$ .

Solution of equation (1) may be written in the form [3]  $c(r, t) = \frac{A}{t^3} \exp \left[ -\frac{r^{2/3}}{\alpha t} \right]$ , where  $\alpha = 4 \left( \frac{\kappa}{9} \right) \cdot \varepsilon^{1/3}$ , and the multiplier  $A$  is determined from the permanence rule for the particle number  $N$  in the whole unrestricted space  $N = \int_0^{\infty} 2\pi r c(r, t) dr$ ,  $A = \frac{N}{2^7 \cdot 3\pi \left( \frac{\kappa}{9} \right)^3 \varepsilon}$ .

Thus, the formula for  $c(r, t)$  can be written in the form

$$c(r, t) = \frac{N}{2^7 \cdot 3\pi \left( \frac{\kappa}{9} \right)^3 \varepsilon t^3} \exp \left[ -\frac{r^{2/3}}{4 \left( \frac{\kappa}{9} \right) \varepsilon^{1/3} t} \right]. \quad (2)$$

Number of particles contained in the cylindrical layer with the radius  $r$  and thickness  $dr$  in the moment of time  $t$  is  $dc = 2\pi r c(r, t) dr$ , and the relation  $2\pi r c(r, t) dr / N = W(r, t) dr$ , where  $W(r, t)$  is the hygroscopic particle distribution probability density, defined by the formula

$$W(r, t) = \frac{r}{2^6 \cdot 3 \left( \frac{\kappa}{9} \right)^3 \varepsilon t^3} \cdot \exp \left[ -\frac{r^{2/3}}{4 \left( \frac{\kappa}{9} \right) \varepsilon^{1/3} t} \right].$$

Herein, average square of the cylinder radius, wherein basic mass of the particles is localized, is

$$\overline{r^2} = \int_0^{\infty} r^2 W(r, t) dr = \frac{1}{3(\alpha t)^3} \cdot \frac{3}{2} (\alpha t)^6 \int_0^{\infty} x^5 e^{-x} dx = \frac{5!}{2} (\alpha t)^3 \approx 5.27 \cdot \varepsilon (\kappa t)^3;$$

hence, the average radius of the expanding cloud of reactive gases is

$$R = \sqrt{r^2} = 2.3\sqrt{\varepsilon}(\kappa t)^{3/2} \sim t^{3/2}. \tag{3}$$

According to the classical formula

$$R = \sqrt{4D_T t} \sim t^{1/2}, \tag{4}$$

where  $D_T$  is the turbulent diffusion coefficient.

Table 1 gives representative values of turbulence parameters in convective clouds borrowed from [2].

Table 2 presents the radius values for the expanding cloud of reactive gases calculated by formulae (2) and (3) inside and below the cloud for *Cu* and *Cb*-hail.

Table 1. Representative values of turbulence parameters in convective clouds.

|                                       | <i>Cu</i>      |           |       |                | <i>Cb</i> - hail |           |                |                |
|---------------------------------------|----------------|-----------|-------|----------------|------------------|-----------|----------------|----------------|
|                                       | inside         | laterally | above | below          | inside           | laterally | above          | Below          |
| $\varepsilon, \text{cm}^2/\text{s}^3$ | $3 \cdot 10^2$ | 2·10      | 2·10  | $1 \cdot 10^2$ | $2.6 \cdot 10^2$ | 4·10      | $1 \cdot 10^2$ | $8 \cdot 10^2$ |
| $D_T, \text{m}^2/\text{s}$            | 70             | 30        | 30    | 50             | 150              | 40        | 50             | 100            |

Table 2. Values of the radius  $R$  of the expanding cloud of reactive gases in different moments of time, m.

| Radius $R$ in different moments of time, m  |               |      |       |       |                            |               |       |       |       |
|---|---------------|------|-------|-------|----------------------------|---------------|-------|-------|-------|
| $R = 2.3\sqrt{\varepsilon}(\kappa t)^{3/2}$ |               |      |       |       | $R = \sqrt{4D_T t}$        |               |       |       |       |
| $\varepsilon, \text{cm}^2/\text{s}^3$       | $t, \text{s}$ |      |       |       | $D_T, \text{m}^2/\text{s}$ | $t, \text{s}$ |       |       |       |
|   | 30            | 60   | 90    | 120   |                            | 30            | 60    | 90    | 120   |
| <i>Cu</i>                                   |               |      |       |       | <i>Cu</i>                  |               |       |       |       |
| Inside<br>$3 \cdot 10^2$                    | 16.7          | 47.3 | 85.1  | 131.0 | Inside<br>70               | 90.0          | 126.6 | 155.2 | 178.8 |
| Below<br>$2 \cdot 10^2$                     | 13.4          | 38.0 | 69.9  | 107.5 | Below<br>30                | 60.0          | 83.0  | 102.0 | 117.0 |
| <i>Cb</i>                                   |               |      |       |       | <i>Cb</i>                  |               |       |       |       |
| Inside<br>$2.6 \cdot 10^2$                  | 15.4          | 43.6 | 80.1  | 123.3 | Inside<br>150              | 134.2         | 190.0 | 232.4 | 268.3 |
| Below<br>$8 \cdot 10^2$                     | 27.0          | 76.5 | 140.5 | 216.4 | Below<br>100               | 109.6         | 155.1 | 190.0 | 219.0 |

One can see from the data of Table 2 that the values of  $R$  calculated inside the cloud by classical formula (4) significantly exceed the values obtained according to the Kolmogorov-Obukhov theory.

Total number of particles  $Q$  contained inside the cloud with the radius  $R$  is

$$Q = \int_0^R 2\pi r c(r, t) dr = \frac{2\pi N}{2^7 \cdot 3\pi (\kappa/9)^3 \varepsilon t^3} \int_0^R r e^{-\frac{r^2}{\alpha t}} dr = \frac{2\pi N}{2^7 \cdot 3\pi (\kappa/9)^3 \varepsilon t^3} \cdot \frac{3}{2} (\alpha t)^3 \int_0^{x_k} x^2 e^{-x} dx = \frac{N}{2} \int_0^{x_k} x^2 e^{-x} dx,$$

where  $x = \frac{r^{3/2}}{\alpha t}$ ,  $x_k = \frac{R^{2/3}}{\alpha t} = \frac{(2.3\sqrt{\varepsilon})^{2/3} \kappa t}{\alpha t} = 3,92$ .

Taking into account that the integral  $\int_0^{3,92} x^2 e^{-x} dx = 1.5$ , we obtain  $Q/N = 0.75$ ; that is,

75% hygroscopic particles forming in the course of reagent dispersion by the rocket method are in a cylinder with the radius  $R$ .

In the classical case this ratio is 0.63; that is, the impurity particles are localized in the expanding volume of the cylindrical form to a lesser extent.

Thus, at turbulent diffusion of aerosol particles from an instantaneous, their basic mass is contained in a cloud with the radius  $R$ . On this basis, thereafter we will assume that the volume containing hygroscopic particles expands by law (3).

### 3. Main stages of expansion of reactive gases of antihail rockets

The process of expansion of reactive gases of antihail rockets may be conventionally divided into several stages.

At the initial stage of the reactive gas cloud expansion its rising takes place, being accompanied by gas cooling due to both involvement of cooler ambient air in it and to evaporation of cloud droplets contained in the cloud air. As certain radius  $R_\kappa$  is achieved, equalization of temperatures inside the cloud and in the ambient environment occurs. For determination of  $R_\kappa$ , we write the equation of heat balance for the expanding cloud of reactive gases

$$\frac{d}{dt}(\rho_i \theta_i R^2) = \rho_e \theta_e \frac{dR^2}{dt} - \frac{L\omega}{c_p} \frac{dR^2}{dt}, \quad (5)$$

where  $\rho_i, \theta_i$  are the density and temperature inside the cloud;  $\rho_e, \theta_e$  are the density and temperature in the cloud environment;  $c_p$  is the specific heat capacity of the gas (air) at constant pressure;  $\omega$  is the absolute water content of the cloud;  $L$  is the specific heat of vapor condensation.

Let us rewrite equation (5) in the form

$$\frac{d}{dz}(\rho_i \theta_i R^2) = \frac{d}{dz}(\rho_e \theta_e R^2) - R^2 \frac{d}{dz}(\rho_e \theta_e) - \frac{L\omega}{c_p} \frac{dR^2}{dz}. \quad (6)$$

As the reactive gas cloud rises at a height of several tens of meters, the product  $\rho_e \theta_e$  does not practically vary. Therefore, neglecting the second summand in the in right-hand member of equation (6) and integrating we obtain

$$\rho_i \theta_i R^2 = \rho_e \theta_e R^2 - \frac{L\omega}{c_p} R^2 + c.$$

Here, the integration constant  $c = \rho_{i0} \theta_{i0} R_0^2$ , where  $\rho_{i0}, \theta_{i0}$  are the density and temperature of reactive gases immediately after their discharge from the rocket nozzle;  $R_0$  is the initial radius of a jet of reactive gases immediately after their discharge from the rocket nozzle. Hence, the value of the cloud radius  $R_\kappa$ , at which the temperature inside the gas and in the ambient environment are equalized, i.e.  $\theta_i = \theta_e$ , is determined from the equation

$$-\frac{L\omega}{c_p} R_\kappa^2 + \rho_{i0} \theta_{i0} R_0^2 = 0,$$

wherefrom we obtain the approximation equation

$$R_\kappa \approx R_0 \left( \frac{\rho_{i0} \theta_{i0} c_p}{L\omega} \right)^{1/2},$$

substituting the representative parameter values here.

For estimation of the  $R_k$  value, we assume that  $c_p = 0.24 \text{ cal/g} \cdot \text{deg}$ ,  $L = 600 \text{ cal/g}$ ,  $\theta_{i0} \approx 3000 \text{ }^\circ\text{C}$ ,  $\rho_{i0} = \frac{p_0}{R_2 T_{i0}} \approx 10^{-4} \text{ g/m}^3$ , where  $p_0$  is the atmospheric pressure,  $R_2$  is the gas constant of reactive gases,  $T_{i0}$  is the temperature, K. Then, we obtain  $R_k \approx 10 \frac{R_0}{\sqrt{\omega}}$ , where  $\omega$  is given in  $\text{g/m}^3$ ,  $R_0 \approx 0.2 \text{ m}$ .

It follows from these estimative calculations that equalization of the temperatures of reactive gases and ambient cloud environment proceed relatively rapidly; in calculation of cloud processes in the zone of hygroscopic nuclei distribution, this process stage can be ignored.

At the second stage of the reactive gas cloud expansion, activity of hygroscopic particles as new nuclei of vapor condensation is exhibited. At first, a film of water is formed on them; its thickness gradually increases until the whole salt crystal is dissolved in the growing droplet. By this moment of time, the radius of the reactive gas cloud achieves the value  $R_1$ . Further expansion of the cloud takes place in conditions of competition for moisture between cloud droplets involved into the reactive gas cloud from the outside and cloud droplets grown on salt particles.

The impact effect of simulated hygroscopic particles introduced into the cloud is determined by character of this competition and possibility of anticipatory appearance of large cloud droplets capable of intense growing due to gravity coagulation.

Thus, expansion of the zone containing reactive gases and simulated hygroscopic particles may be conventionally divided into three stages:

1.  $R_0 < R \leq R_k$  - salt particles act passively;
2.  $R_k < R < R_1$  - salt particles dissolve inside the droplets that are formed on them;
3.  $R \geq R_1$  - the cloud environment contains natural cloud droplets and "salt" droplets that are in competition for moisture.

As it is known, humidity for dissolution of pure *NaCl* is 75.3% (for *KCl* it is 84.3%). Therefore, at air humidity exceeding 75.3% water vapor condensates on *NaCl* particles. With the course of time, the salt crystal surface is coated with a film of salt water; a cloud droplet is formed, inside of which the crystal is dissolved. As the droplet achieves certain dimension, the crystal in it entirely dissolves.

Kinetics of the process of the salt particle dissolution inside the droplet with fixed radius value was considered in [4] in the approximate statement of the problem.

Here we consider the simplified variant of this problem solution taking into account the condensation growth of droplets.

The representative time  $\tau_1$  of formation of a cloud droplet with the radius  $r$  due to vapor condensation is on the order of  $\tau_1 \sim \frac{r^2}{D} \frac{\rho_l}{\Delta\rho_v}$ , where  $D$  is the coefficient of vapor diffusion in

air,  $\rho_l$  is the water density,  $\Delta\rho_v = \rho_{v\infty} - \rho_{vh}$ ,  $\rho_{v\infty}$  is the vapor density far off the droplet;  $\rho_{vh}$  is the saturating vapor density on its surface. The representative time of equilibrium salt concentration settling in the droplet is  $\tau_2 \sim \frac{r^2}{D_1}$ , where  $D_1$  is the coefficient of salt ion diffusion in

water. The relation is  $\frac{\tau_2}{\tau_1} \approx \frac{D}{D_1} \cdot \frac{\Delta\rho_v}{\rho_l}$ . Substituting here  $D \approx 0.1 \text{ cm}^2/\text{s}$ ,  $D_1 \approx 1 \cdot 10^{-5} \text{ cm}^2/\text{s}$ ,

$\frac{\Delta\rho_v}{\rho_l} \approx 10^{-6}$ , we obtain  $\tau_2/\tau_1 \approx 10^{-2}$ .

It follows from these estimations that in the process of condensation growth of cloud droplets on salt particles, the solution concentration in the droplet remains all the while close to equilibrium, until the salt particle is entirely dissolved.

For solution of the problem of salt crystal dissolution in the droplet, we assume that the crystal is shaped as a sphere and is situated in the droplet center. Herein, the law of variation of the crystal mass  $m_k$  can be written as  $\frac{dm_k}{dt} = -c_H \frac{dm}{dt}$ , where  $m$  is the droplet mass,  $c_H$  is the saturating concentration of salt solution in water. Hence, we obtain

$$\frac{dr_k^3}{dt} = -\frac{\rho_{\text{жс}} c_H}{\rho_k} \frac{dr^3}{dt}, \quad (7)$$

where  $\rho_k$  is the density of the salt crystal,  $r_k$  is its radius.

The law of growth of the droplet mass  $m$  in the course of condensation growth is described by the equation

$$\frac{dm}{dt} = 4\pi r D [\rho_{v\infty} - \rho_{vr} (1 - c_H)], \quad (8)$$

where  $\rho_v$  is the saturating vapor density above the droplet surface.

The heat balance equation on the droplet surface has the form

$$L \frac{dm}{dt} = 4\pi \lambda r (T_r - T), \quad (9)$$

where  $\lambda$  is the air heat conduction coefficient,  $T$  is the absolute temperature of the ambient environment,  $T_r$  is the droplet surface temperature.

From equations (8) and (9) we obtain

$$T_r - T = \frac{LD}{\lambda} [\rho_{v\infty} - \rho_{vr} (1 - c_H)]. \quad (10)$$

Here  $\rho_{vr} = \frac{E(T_r)}{R_n T}$ , where  $R_n$  is the gas constant of water vapor,  $E(T_r)$  is the saturating vapor pressure above the surface of a droplet with the radius  $r$ , which is related to the saturating vapor pressure above the flat surface of pure water  $E_\infty(T_r)$  by the known Kelvin formula

$$E(T_r) = \left(1 + \frac{2\sigma}{\rho_l R_n T r}\right) E_\infty(T_r),$$

where  $\sigma$  is the water surface tension. Herein, from the Clapeyron-Clausius equation we obtain

$$E_\infty(T_r) = E(T) \exp\left[1 + \frac{L(T_r - T)}{R_n T^2}\right],$$

hence,

$$\rho_{vr} = \rho_{vh}(T) \left(1 + \frac{2\sigma}{\rho_l R_n T r}\right) \cdot \left[1 + \frac{L(T_r - T)}{R_n T^2}\right], \quad (11)$$

where  $\rho_{vh}(T) = \frac{E(T)}{R_n T}$  is the saturating vapor density at the temperature  $T$ . After substitution of (11) in (10) we find

$$T_r - T = \frac{\rho_{\infty} - \rho_{vh}(1 - c_h) \left(1 + \frac{2\sigma}{\rho_l R_n T r}\right)}{\frac{\lambda}{LD} + \frac{L\rho_{vh}}{R_n T^2} \left(1 + \frac{2\sigma}{\rho_l R_n T r}\right) (1 - c_h)}.$$

Equation (8) takes the form

$$r \frac{dr}{dt} = \frac{D}{\rho_l} \cdot \frac{\rho_{\infty} - \rho_{vh}(1 - c_h) \left(1 + \frac{2\sigma}{\rho_l R_n T r}\right)}{1 + \frac{\rho_{vh} D L^2}{\lambda R_n T^2} \left(1 + \frac{2\sigma}{\rho_l R_n T r}\right) (1 - c_h)}. \quad (12)$$

Estimations show that for salt crystals with  $r_k > 10^{-6}$  m the value  $2\sigma/\rho_l R_n T r \ll 1$ , and equation (12) is significantly simplified

$$r \frac{dr}{dt} = \frac{D}{\rho_l} \cdot \frac{\rho_{\infty} - \rho_{vh}(1 - c_h)}{1 + \frac{\rho_{vh} D L^2}{\lambda R_n T^2} (1 - c_h)}, \quad t \leq \tau, \quad (13)$$

where  $\tau$  is the time of entire dissolution of the salt crystal in water.

It follows from equation (13) that the droplet containing the salt crystal will grow provided that  $\rho_{\infty} > \rho_{vh}(1 - c_h)$ , i.e., even in conditions of undersaturation in the ambient cloud environment.

Integrating equation (13) and taking into account that  $r = r_{k0}$  at  $t = 0$ , where  $r_{k0}$  is the initial radius of the salt crystal, we will obtain

$$r = r_{k0} \left(1 + \frac{2aD}{\rho_l r_{k0}^2} t\right)^{1/2} \quad t \leq \tau, \quad (14)$$

where

$$a = \rho_{vh} \frac{f - 1 + c_h}{1 + \frac{\rho_{vh} L^2 D}{\lambda R_n T^2} (1 - c_h)},$$

where  $f$  is the relative humidity of air.

Substituting (14) in equation (7) and integrating, we come to the formula defining the law of the salt crystal dissolution in the droplet

$$r_k = r_{k0} \left[1 + \frac{2aD}{\rho_l r_{k0}^2} - \frac{2aD}{\rho_l r_{k0}^2} \left(1 + \frac{2aDt}{\rho_l r_{k0}^2}\right)^{3/2}\right]^{1/3}. \quad (15)$$

Assuming that  $r_k = 0$ , we find the entire salt dissolution time  $\tau$

$$\tau = \frac{\rho_l r_{k0}^2}{2aD} \left[ \left(1 + \frac{\rho_k}{\rho_l c_h}\right)^{2/3} - 1 \right]. \quad (16)$$

For  $NaCl$  the expression in square brackets is 2.687; therefore,  $\tau = 1.34 \frac{\rho_l r_{k0}^2}{aD}$ .

Substituting the obtained value of  $\tau$  instead of  $t$  in equation (14), we find the droplet radius  $r_0$  in the moment of entire dissolution of the salt particle

$$r_0 = r_{\kappa 0} \left( 1 + \frac{\rho_{vh}}{\rho_l c_h} \right)^{1/3} = 1.9 r_{\kappa 0}.$$

Table 3 presents the time of entire dissolution of *NaCl* particles with different radii in the growing cloud droplet in conditions of undersaturation ( $f = 0.9$ ) and total saturation ( $f = 1$ ) of the ambient air.

Table 3. Time of entire dissolution of *NaCl* salt crystals in cloud droplets.

| $r_{\kappa 0}$ , cm |           | $1 \cdot 10^{-5}$   | $5 \cdot 10^{-5}$   | $1 \cdot 10^{-4}$   | $5 \cdot 10^{-4}$ | $1 \cdot 10^{-3}$ |
|---------------------|-----------|---------------------|---------------------|---------------------|-------------------|-------------------|
| $\tau$ , s          | $f = 0,9$ | $4.2 \cdot 10^{-4}$ | $1.1 \cdot 10^{-2}$ | $4.2 \cdot 10^{-2}$ | 1.1               | 4.2               |
|                     | $f = 1$   | $6 \cdot 10^{-4}$   | $1.5 \cdot 10^{-2}$ | $6 \cdot 10^{-2}$   | 1.5               | 6.0               |

One can see from the data of Table 3 that in calculation of the condensation growth of cloud droplets on *NaCl* crystals with radii up to  $10 \mu\text{m}$ , the stage of salt particle dissolution in droplets may be ignored, and one can start the calculations assuming that the initial radius of “salt” cloud droplets is  $r_0 = 1.9 r_{\kappa 0}$ ; at  $r_{\kappa 0} > 10 \mu\text{m}$  equation (13) must be included into the calculation model.

After entire dissolution of the salt crystal in water, its further growth is determined by equation (13), wherein the constant  $c_h$  is substituted by the variable concentration  $c$ , which is defined by the formula  $c = c_h \left( \frac{r_0}{r} \right)^3$ . Herein, we obtain

$$r \frac{dr}{dt} = \frac{D}{\rho_l} \cdot \frac{\rho_{v\infty} - \rho_{vh} \left[ 1 - c_h \left( \frac{r_0}{r} \right)^3 \right]}{1 + \frac{\rho_{vh} D L^2}{\lambda R_n T^2} \left[ 1 - c_h \left( \frac{r_0}{r} \right)^3 \right]}. \tag{17}$$

Figure 1 shows curves of the condensation growth of cloud droplets on *NaCl* crystals at air humidity being less than the saturating one.

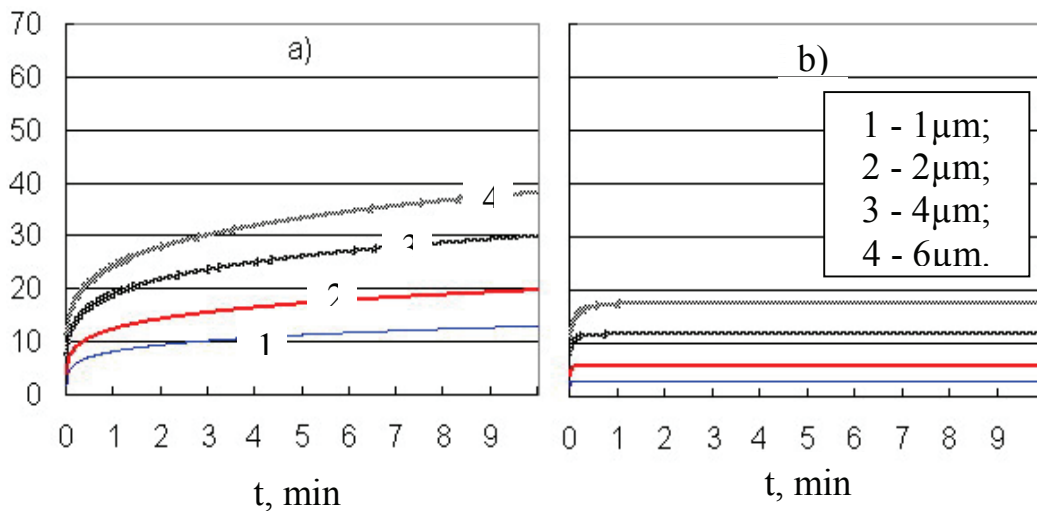


Fig. 1. Curves of condensation growth of cloud droplets on *NaCl* crystals below the cloud: (a) the cloud humidity of 100% ( $f = 1$ ); (b) the cloud humidity of 90% ( $f = 0.9$ ).



One can see from the figure that after introduction of salt particles under the cloud base, where air is not saturated as yet, large cloud droplets appear, which being entrained by an up-draft into the cloud volume, can grow further due to coagulation with natural cloud droplets and so they can anticipatorily initiate the precipitation formation process.

Figure 2 presents curves of cloud droplet growth on *NaCl* salt particles at air oversaturations being characteristic of cumulus clouds. The figure data show that “salt” drops grow appreciably more rapidly than natural cloud droplets; for several minutes they achieve radii of 20-30  $\mu\text{m}$ , at which intense growth of the coagulation process begins.

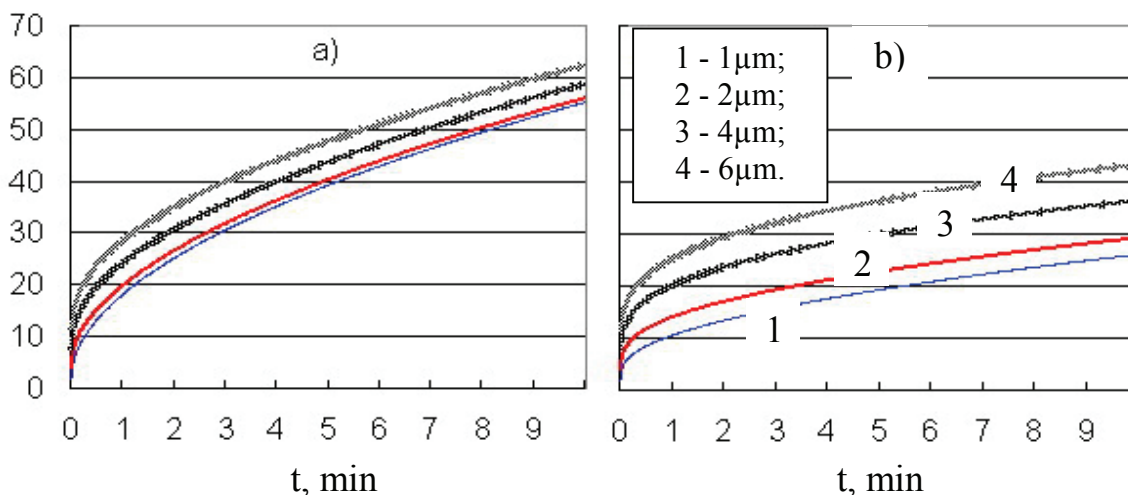


Fig. 2. Curves of condensation growth of cloud droplets on *NaCl* crystals inside the cloud: (a) oversaturation of 5% ( $f=1.05$ ); (b) oversaturation of 1% ( $f=1.01$ ).

Thus, on the basis of the data of Figs. 1 and 2, we can make a preliminary conclusion that for hygroscopic impact on convective clouds, it is efficient to introduce salt particles in the lower cloud base.

This work was partially financed in the framework of the Academy of Sciences of Moldova and Russian Foundation for Basic Research cooperation research project.

### References

- [1] M.T. Abshaev, N.I. Mikheev, D.V. Kratirov, V.A. Zorin, A.P. Talalaev, and B.K. Kuznetsov, *Novaya raketa dlya aktivnykh vozdystvii na oblaka*, Tezisy Vseros. Konf. po fizike oblakov i aktivnym vozdystviyam na gidrometeor. protsessy, Nalchik, 28, (2005).
- [2] I.P. Mazin, and A.H. Hrgian, *Oblaka i oblachnaya atmosfera*, Leningrad, Gidrometeoizdat, 647, 1989.
- [3] E.N. Parker, *Dinamicheskie protsessy v mezplanetnoi srede*, Moscow, Mir, 362, 1965.
- [4] Yu.P. Sedunov, *Fizika obrazovaniya zhidko-kapel'noi fazy v atmosfere*, Leningrad, Gidrometeoizdat, 207, 1972.
- [5] Report of the WMO International Workshop on Hygroscopic Seedings: experimental results, physical processes, and research needs. Edited by G. Brant Foote and Roelof T. Bruintjes; Mexico; National Centre for Atmospheric Research, USA. - [Geneva: WMO, 2000]. (Series: Weather Modification Programme (WMP); Report no. 35. WMO; TD no. 1006). 67 p. Call no: WMP 35 TD 1006.
- [6] Report of the Meeting of Experts on Hail Suppression: Efficacy, Evaluation and New Developments in HS Methods. Edited by Rumien D. Bojkov and G. Brant Foote; Organized by WMO in collaboration with Roshydromet; Nalchik, 27 September – 2 October 2003 Russia, - [Geneva: WMO, 2004]. (Series: Weather Modification Programme (WMP); Report no. 41. WMO; TD no. 1233). 167 p. Call no: WMP 41 TD 1233.